Bioresource Technology 224 (2017) 670–679

Contents lists available at ScienceDirect

Bioresource Technology

journal homepage: www.elsevier.com/locate/biortech

Energy efficient bead milling of microalgae: Effect of bead size on disintegration and release of proteins and carbohydrates

P.R. Postma [a,*,1], E. Suarez-Garcia [a,1], C. Safi [b], K. Yonathan [a], G. Olivieri [a,c], M.J. Barbosa [a], R.H. Wijffels [a,d], M.H.M. Eppink [a]

[a] Bioprocess Engineering, AlgaePARC, Wageningen University & Research, PO Box 16, 6700 AA Wageningen, The Netherlands
[b] Wageningen Food & Biobased Research, AlgaePARC, PO Box 17, 6700 AA Wageningen, The Netherlands
[c] Dipartimento di Ingegneria Chimica, dei Materiali e della Produzione Industriale, Università degli Studi di Napoli Federico II, Piazzale V. Tecchio 80, 80125 Napoli, Italy
[d] Nord University, Faculty of Biosciences and Aquaculture, N-8049 Bodø, Norway

HIGHLIGHTS

- Bead milling is an energy efficient and mild microalgae disintegration method.
- A smaller bead size results in a lower specific energy consumption.
- The specific energy consumption was decreased from >1.7 to <0.5 kWh kg_{DW}^{-1}.
- Product yields were unaffected using smaller bead sizes.

ARTICLE INFO

Article history:
Received 12 October 2016
Received in revised form 16 November 2016
Accepted 17 November 2016
Available online 19 November 2016

Keywords:
Bead milling
Bead size
Microalgae
Energy
Stress parameters
Protein release

ABSTRACT

The disintegration of three industry relevant algae (*Chlorella vulgaris*, *Neochloris oleoabundans* and *Tetraselmis suecica*) was studied in a lab scale bead mill at different bead sizes (0.3–1 mm). Cell disintegration, proteins and carbohydrates released into the water phase followed a first order kinetics. The process is selective towards proteins over carbohydrates during early stages of milling. In general, smaller beads led to higher kinetic rates, with a minimum specific energy consumption of $\leqslant$0.47 kWh kg_{DW}^{-1} for 0.3 mm beads. After analysis of the stress parameters (stress number and stress intensity), it appears that optimal disintegration and energy usage for all strains occurs in the 0.3–0.4 mm range. During the course of bead milling, the native structure of the marker protein Rubisco was retained, confirming the mildness of the disruption process.

1. Introduction

There is a growing demand for sustainable protein sources and bio-based products as an alternative for traditional agricultural crops. Microalgae are a potential source of renewable high value proteins, carbohydrates, lipids and pigments for food, feed and chemical industries (Vanthoor-Koopmans et al., 2013). Such products are typically located intracellular, either in the cytoplasm, in internal organelles or bound to cell membranes, and in most cases, the cells need to be disintegrated before extraction. This step can be done by chemical hydrolysis (Safi et al., 2014), high pressure homogenization (Safi et al., 2014), ultrasonication (Grimi et al., 2014), pulsed electric fields (Goettel et al., 2013; Grimi et al., 2014; Postma et al., 2016) or bead milling (Doucha and Lívanský, 2008; Günerken et al., 2015; Montalescot et al., 2015; Postma et al., 2015).

Bead mills are commonly applied in the chemical industry for the manufacture of paints/lacquers and grinding of minerals (Kula and Schütte, 1987) and have been successfully applied for the disintegration of yeast (Bunge et al., 1992), cyanobacteria (Balasundaram et al., 2012) and microalgae (Günerken et al., 2016; Postma et al., 2015) for the release of intracellular products, under low energy inputs and mild conditions. The efficiency of cell disintegration in bead mills depends on several parameters such as chamber and agitator geometry, biomass concentration, agitator speed (i.e., tip speed of agitator), suspension flow rate, bead filling ratio, bead type and bead diameter. A high bead filling ratio (>55% v/v) was found to be optimal for disruption according to

* Corresponding author.
E-mail address: richard.postma@wur.nl (P.R. Postma).
[1] Both authors contributed equally to this work.

http://dx.doi.org/10.1016/j.biortech.2016.11.071
0960-8524/

Abbreviations

A	peak area [AU]
C	constant [–]
C_i	concentration of component i in supernatant [g L^{-1}]
$C_{i,Biomass}$	total concentration of component i in biomass [g L^{-1}]
C_V	volume cell concentration [–]
d_b	bead diameter [m]
E_M	specific energy consumption [kWh kg_{DW}^{-1}]
$\tilde{E}_M$	theoretical specific energy consumption [kWh kg_{DW}^{-1}]
$E_{M,3\tau}$	specific energy consumption at 3τ [kWh kg_{DW}^{-1}]
$E_{M,min}$	minimal specific energy consumption [kWh kg_{DW}^{-1}]
k_{carb}	carbohydrate release first order kinetic constant [s^{-1}]
k_{dis}	disintegration first order kinetic constant [s^{-1}]
k_{prot}	protein release first order kinetic constant [s^{-1}]
M	mass of biomass on dry weight [kg]
n	agitator speed (revolutions) [s^{-1}]
SN	stress number [–]
SN_D	reduced Stress number for disintegration [–]
SN_G	reduced Stress number for grinding [–]
SI	stress intensity [J/Nm]
SI_{opt}	optimal stress intensity [J/Nm]
t	disruption/milling time [s]
u_s	agitator tip speed [m s^{-1}]
V	volume [mL]
X_i	degree of disintegration (Dis), protein concentration or carbohydrate concentration [–]
$X_{i,max}$	maximal degree of disintegration (Dis), protein concentration or carbohydrate concentration [–]
Y_{carb}	carbohydrate yield [%]
Y_{prot}	protein yield [%]
ε	bead bulk density [kg m^{-3}]
φ_b	bead filling ratio [–]
ρ_b	specific density beads [kg m^{-3}]
τ	characteristic time of process kinetic [s]

Montalescot et al. (2015). In addition, Doucha and Lívanský (2008) found that zirconium oxide (ZrO_2) beads are more efficient than glass beads because of their higher specific density. Postma et al. (2015) investigated the disintegration of *C. vulgaris* by bead milling at lab scale using ZrO_2 beads with a diameter of 1 mm (65% v/v bead filling) and found that an agitator speed u_s of 6 m s^{-1} provides a lower specific energy consumption; though with a biomass concentration of 145 g kg_{DW}^{-1} a lower specific energy input could be obtained, a concentration of 87.5 g kg_{DW}^{-1} showed to have a better biomass suspension handling and higher protein yields.

Furthermore, for the disintegration of the microalga *Chlorella* sp. it was found that similar specific energy consumptions were achieved for the same flow rate, biomass concentration and agitator speed for beads of 0.3–0.4 and 0.6–0.8 mm (Doucha and Lívanský, 2008). On the other hand, the disintegration of the microalga *Scenedesmus* sp. and *Nannochloropsis oculata* was improved when smaller beads (0.35–0.6 mm) were applied (Hedenskog et al., 1969; Montalescot et al., 2015).

Bunge et al. (1992) studied the release of enzymes from *Arthrobacter* by means of bead milling. It was found that small glass beads (Ø 0.205–0.460 mm) at moderate to high biomass concentrations and low to moderate agitator speeds result in optimal energy utilization. Schütte et al. (1983) found that smaller beads (0.55–0.85 mm) are more beneficial to release intracellular products from the cytoplasm of yeast over larger beads (1 mm). On the other hand, the larger beads are better at releasing products from the periplasm.

To describe the comminution of cells in bead mills as a function of different process parameters, Kwade and Schwedes (2002) and Bunge et al. (1992) presented a very clear description of the so-called Stress Model (SM). The SM assumes that the disruption process in stirred media mills (e.g., bead mill) is governed by the number of stress events (i.e., bead to bead collisions) and by the intensity of such events. Quantitatively, this is expressed by the Stress Number (SN) (Eqs. (1) and (2)) and the Stress Intensity (SI) (Eq. (4)) (Bunge et al., 1992; Kwade and Schwedes, 2002); two types of behaviors are also recognized: 1) disintegration/deagglomeration of cells, characterized by the fact that a cell is either intact or disrupted; and 2) grinding of crystalline materials, applicable for materials in which the particle size decreases during the milling process.

Accordingly, the SN (–) can be calculated for Disintegration (SN_D) and for Grinding (SN_G) as:

$$SN \propto \frac{\varphi_b(1-\varepsilon)}{\{1-\varphi_b(1-\varepsilon)\}c_V}\frac{nt}{d_b} \propto C \cdot SN_D \tag{1}$$

$$SN \propto \frac{\varphi_b(1-\varepsilon)}{\{1-\varphi_b(1-\varepsilon)\}c_V}\frac{nt}{d_b^2} \propto C \cdot SN_G \tag{2}$$

with

$$C = \frac{\varphi_b(1-\varepsilon)}{\{1-\varphi_b(1-\varepsilon)\}c_V} \tag{3}$$

where φ_b is the bead filling ratio (–), ε is the bead bulk porosity (–), c_V the volume cell concentration (–), n the agitator revolutions (s^{-1}), t the milling time (s) and d_b the bead diameter (m).

Furthermore, the SI (Nm) can be regarded as the magnitude of the kinetic energy of a single bead and can be calculated as:

$$SI \propto d_b^3 \rho_b u_s^2 \tag{4}$$

in which ρ_b is the specific density of the beads (kg m^{-3}) and u_s is the agitator tip speed (m s^{-1}). A cell can only be intact or disintegrated upon the release of the intracellular products. Therefore, an optimal stress intensity SI_{opt} can be considered. At or above SI_{opt} cells break with a single stress event; below SI_{opt}, multiple stress events are required to break the cell.

Consequently, the theoretical specific energy input is proportional to the product of the number of stress events times the energy of such events:

$$\tilde{E}_M \propto \frac{SN \cdot SI}{M} \tag{5}$$

where M is the mass of biomass (kg_{DW}) in the system and $\tilde{E}_M$ is the theoretical specific energy input (kWh kg_{DW}^{-1}).

The SM was first applied to microalgae by Montalescot et al. (2015). However, to our knowledge, it has not been applied in combination with the release of water soluble microalgae components. In large scale disruption trials for yeasts and bacteria, Schütte et al. (1983) observed that cytoplasmic enzymes were better solubilized by smaller beads, and that periplasmic enzymes were more easily released by larger beads. We therefore hypothesize that smaller beads could interact more effectively with internal organelles over larger beads and thus are better able to release proteins (e.g., Rubisco) from the pyrenoids and carbohydrates from the cell wall or starch granules. If the process is operated above SI_{opt}, smaller

beads would also lead to higher kinetics, higher yields and lower energy consumption.

The aim of this work is to investigate the effect of the bead size on the disintegration, release of water soluble components and energy consumption during the bead milling of *C. vulgaris*, *N. oleoabundans* and *T. suecica*.

2. Methods

2.1. Microalgae, cultivation and harvesting

Chlorella vulgaris (SAG 211-11b, EPSAG Göttingen, Germany) was cultivated according to Postma et al. (2016).

Neochloris oleoabundans (UTEX 1185, University of Texas Culture Collection of Algae, USA) was cultivated using a fully automated 1400 L vertical stacked tubular photo-bioreactor (PBR) located in a greenhouse (AlgaePARC, The Netherlands). The algae were cultivated in Bold's Basal medium (CCAP, 2015) at a pH value of 8.0 and the temperature was controlled at 30 °C. The light intensity was set at an average of 400 μmol m^{-2} s^{-1}.

Tetraselmis suecica (UTEX LB2286, University of Texas Culture Collection of Algae, USA) was cultivated in repeated batches in a 25 L flat panel PBR (AlgaePARC, The Netherlands) at 20 °C. Ten fluorescent lamps (Philips 58 W/840) provided a continuous incident light intensity of 373 μmol m^{-2} s^{-1}. The PBR was located in a greenhouse and thus, it was also exposed to natural light during the period October 2015–January 2016 (Wageningen, The Netherlands). Mixing and pH control (pH 7.5) were provided by sparging gas (0.254 vvm) composed of a mix of air and 5% v/v CO_2. Walne medium was supplied at a ratio of 8.8 mL L^{-1} medium (Michels et al., 2014).

To obtain a biomass paste, *C. vulgaris* was centrifuged (4000×*g*, 15 min) using a swing bucket centrifuge (Allegra X-30R, Beckman Coulter, USA) while *N. oleoabundans* and *T. suecica* were centrifuged (80 Hz, ~3000×*g*, 0.75 m^3 h^{-1}) using a spiral plate centrifuge (Evodos 10, Evodos, The Netherlands). After centrifugation, the biomass paste of all three algae was stored at 4 °C in the dark and used within two days. Prior to disintegration experiments, the biomass paste was resuspended in phosphate-buffered saline (PBS) (1.54 mM KH_2PO_4, 2.71 mM $Na_2HPO_4{\cdot}2\ H_2O$, 155.2 mM NaCl at pH 7.0) to obtain a biomass concentration (C_x) of about 90 g kg^{-1}. C_x is expressed as g dried biomass per kg algae suspension.

2.2. Bead mill experimental procedure

The bead mill experiments were performed in a horizontal stirred bead mill (Dyno-Mill Research Lab, Willy A. Bachofen AF Maschinenfabrik, Switzerland) operated in batch recirculation mode. The operation procedure was previously described by Postma et al. (2015). In brief, the mill consists of a milling chamber ($V_{chamber}$ 79.6 mL) in which the beads are accelerated by a single DYNO®-accelerator (Ø 56.2 mm). To maintain the feed temperature at 25 °C, a cooling water bath connected to a cooling jacket integrated in the milling chamber and a cooling coil in the feed funnel were used. Yttrium stabilized ZrO_2 beads (Tosoh YTZ®) with four diameters (0.3, 0.4, 0.65 and 1 mm, specific density ρ_b of 6 g cm^{-3}, bulk density ε of 3.8 g cm^{-3}) were applied. The beads were loaded at a constant filling volume of 65% v/v.

First order release kinetics was used to calculate the kinetic constant k_i for the disintegration percentage (k_{dis}), protein release (k_{prot}) or carbohydrate release (k_{carb}) as:

$$\frac{X_i(t)}{X_{i,max}} = 1 - e^{-k_i \cdot t} \tag{6}$$

where $X_i(t)$ represents the degree of disintegration (Dis), the protein concentration or the carbohydrate concentration at time t, and $X_{i,max}$ represents the maximal degree of disintegration, protein concentration or carbohydrate concentration in the liquid phase.

Upon reviewing our previous work (Postma et al., 2015), an error in the calculation of the residence time was noticed. The bead bulk density ε was not correctly incorporated, leading to an underestimation of the free volume in the milling chamber. The residence time t_r should be recalculated as:

$$t_r = t \cdot \frac{V_{Chamber,free}}{V_{total}} \tag{7}$$

with

$$V_{Chamber,free} = V_{Chamber} \cdot \frac{\varepsilon}{\rho_b} \cdot \varphi_b \tag{8}$$

in which t is the batch disintegration time, $V_{Chambe,free}$ represents the volume inside the chamber filled with algae suspension (46.8 mL) and V_{total} (~185 mL) is the total batch volume. $V_{Chamber}$ is the milling chamber volume (79.6 mL), ε is the bead bulk density (3.8 kg m^{-3}), ρ_b is the specific density (6.0 kg m^{-3}) and φ_b is the bead filling ratio (0.65). For a correct comparison of the kinetic data in this work with the previous publication (Postma et al., 2015), the kinetic data and doubling times of the previous work (Postma et al., 2015) have to be multiplied and divided by a factor 0.595, respectively.

2.3. Analytical methods

2.3.1. Sample collection

Samples were taken at different time intervals directly from the feeding funnel, which was maintained under gentle stirring. The maximum sampled volume was always <2.5% of the feed volume. For all cases, bead milling experiments were conducted for 1 h (batch processing time).

2.3.2. Biomass quantification

The dry weight concentration was determined as described by Lamers et al. (2010). The DW/OD_{750} ratio for *C. vulgaris*, *N. oleoabundans* and *T. suecica* were determined experimentally to be 0.312, 0.350 and 0.537, respectively. These ratios were used to calculate the initial biomass concentration. The cell size and cell number were measured with a cell counter (Beckman Coulter Multisizer 3, USA). The samples were diluted using Coulter® Isoton® II dilution buffer. The cell size and cell number were used to calculate the total cell volume.

2.3.3. Disintegration, protein and carbohydrate analysis

The disintegration percentage was analyzed as described by Postma et al. (2015), protein analysis on dry weight (DW) and the water soluble protein after bead milling were analyzed as described by Postma et al. (2015) according to the method developed by Lowry et al. (1951). The carbohydrate content on DW and the water soluble carbohydrates after bead milling were determined as described by Postma et al. (2016) according to the method developed by DuBois et al. (1956).

The protein and carbohydrate yield after bead milling are expressed as:

$$Y_i = \frac{C_i(t) - C_i(0)}{C_{i,Biomass}} \tag{9}$$

where $C_i(t)$ and $C_i(0)$ are the concentrations of component i in the supernatant at time t and 0, respectively. $C_{i,Biomass}$ is the total content of component i within the total biomass (DW), where i can be protein or carbohydrates.

2.3.4. Starch analysis

To determine the total starch content on biomass DW, lyophilized algae were dissolved in 1 mL 80% ethanol and bead beated at 6000 RPM for 3 cycles with 120 s breaks in between cycles, after which the total starch content was determined using a commercial kit (Total Starch, Megazyme International, Ireland). The absorbance was measured at a wavelength of 510 nm with a spectrophotometer (DR6000, Hach Lang, USA).

2.3.5. Scanning electron microscopy

150 µL microalgae suspension was applied on poly-L-lysine coated cover slips (Ø 8 mm) and incubated for 1 h. Subsequently the samples were rinsed in fresh PBS and fixed for 1 h in 3% glutaraldehyde in PBS. After washing twice in PBS, the samples were post-fixed in 1% OsO_4 for one hour, rinsed with demineralized water and dehydrated in a graded (30-50-70-90-100-100%) ethanol series. Subsequently, the samples were critical point dried with CO_2 (EM CPD 300, Leica, Wetzlar, Germany). The cover slips were attached to sample holders using carbon adhesive tabs (EMS, Washington, USA) and sputter coated with 10 nm Wolfram (EM SCD 500, Leica, Wetzlar, Germany). The samples were analyzed in a high resolution scanning electron microscope at 2 kV at room temperature (Magellan 400, FEI, Eindhoven, The Netherlands). Images were contrast enhanced with Photoshop CS5.

2.3.6. Native PAGE analysis

Native PAGE analysis was performed as described by Postma et al. (2016). In addition, scanned gels were analyzed by ImageJ (IJ 1.46r) to convert the Rubisco band intensity in a density chromatogram. Subsequently, the chromatogram was integrated. From the peak areas, the relative density was determined over the course of bead milling:

$$Relative\ density(-) = \frac{A_{Peak,final}}{A_{Peak,t}} \quad (10)$$

where $A_{Peak,final}$ is the peak area of Rubisco in the final sample and $A_{Peak,t}$ the peak area of Rubisco at time t.

2.4. Statistical analysis

Statistical analysis was performed by analysis of variance (ANOVA). When groups were significantly different at an α level of 0.05, Tukey's honest significance test was performed to find which groups differed.

3. Results and discussion

The overall effect of bead size is studied first in terms of kinetic rates and product yields. The mechanism of disintegration is then analyzed using the stress model and subsequently the specific energy consumption and selective protein release are presented.

3.1. Disintegration and product release kinetics

As a follow up to Postma et al. (2015), in which a benchmark for the disintegration of *C. vulgaris* using 1 mm ZrO_2 beads was proposed, one goal of this study was to evaluate the effect of decreasing the bead size during bead milling of microalgae.

Fig. 1 shows the fraction of cell disintegration, protein and carbohydrate release for *T. suecica* for 0.3 mm beads. It can be observed that a disintegration percentage and protein release of over 99% can be reached in a total processing time of 400 s. Nevertheless, the maximal amount of carbohydrate was only found at the end of the experiment without reaching a plateau. For the other bead sizes and algae species, disintegration percentages

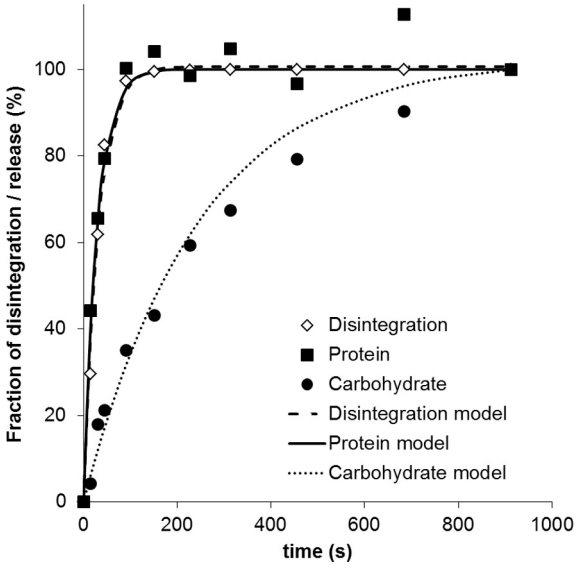

Fig. 1. Relative disintegration and release of protein and carbohydrate for *T. suecica* using 0.3 mm beads.

>99% were obtained. By means of Least Square Error Regression (LSER) the first order model (Eq. (6)) was fitted to the experimental disintegration percentage, protein and carbohydrate release data. In all cases, the coefficient of correlation ranged between 0.8856 and 0.9997.

Fig. 2A–C presents an overview of kinetics constants for disintegration, proteins and carbohydrates release, respectively, for all algae strains and bead sizes. *Chlorella vulgaris* showed a clear optimum bead size of 0.4 mm for disintegration and release of carbohydrates. The k_{dis} of 0.041 ± 0.003 s^{-1} from this study represents a significant fourfold increase ($p < 0.05$) with respect to the benchmark of 1 mm beads (k_{dis} = 0.009 ± 0.001 s^{-1}). The protein release constant (Fig. 2B) using the 1 mm beads was similar to the previously determined benchmark (Postma et al., 2015). It can be observed that *C. vulgaris* shows an increasing trend in the protein release rate for a decreasing bead size.

For *N. oleoabundans* a clear upward trend in the k_{dis} and k_{prot} was observed when decreasing the bead size, but no evident optimum bead size appeared. The best disintegration results obtained with a k_{dis} of 0.025 ± 0.001 s^{-1} was 3-fold faster using 0.3 mm beads than the 1 mm beads. The carbohydrate release for *N. oleoabundans* did not show significant differences (p = 0.44). *Neochloris oleoabundans* and *C. vulgaris* exhibit several structural similarities, including cell size (average 3.3 µm and 3.2 µm, respectively) and morphology. Yet, we observed different kinetic constants, in particular, for carbohydrates. This is most likely caused by differences in the cell composition and cell wall structure of both algae, which contain cellulose-like polymer structures. The genus *Chlorella* is known to have amino sugars as constituents in the rigid cell wall, and it is suspected that chitin-like glycans are present (Kapaun and Reisser, 1995). To our knowledge, no literature exists on the polymeric links present in *N. oleoabundans*.

Among the strains tested, the disintegration rates of *T. suecica* were higher, and statistically independent of bead size. This clearly suggests a weaker cell structure (Kermanshahi-pour et al., 2014). A maximum k_{dis} of 0.050 ± 0.009 s^{-1} was determined, which is almost fivefold higher than the rates for *C. vulgaris* and *N. oleoabundans* (1 mm beads), but only 60% of the rate obtained by Halim et al. (2013) when disrupting *T. suecica* using ultrasound for similar batch volume and processing time. No significant trend was observed in the protein or carbohydrate release rate with respect

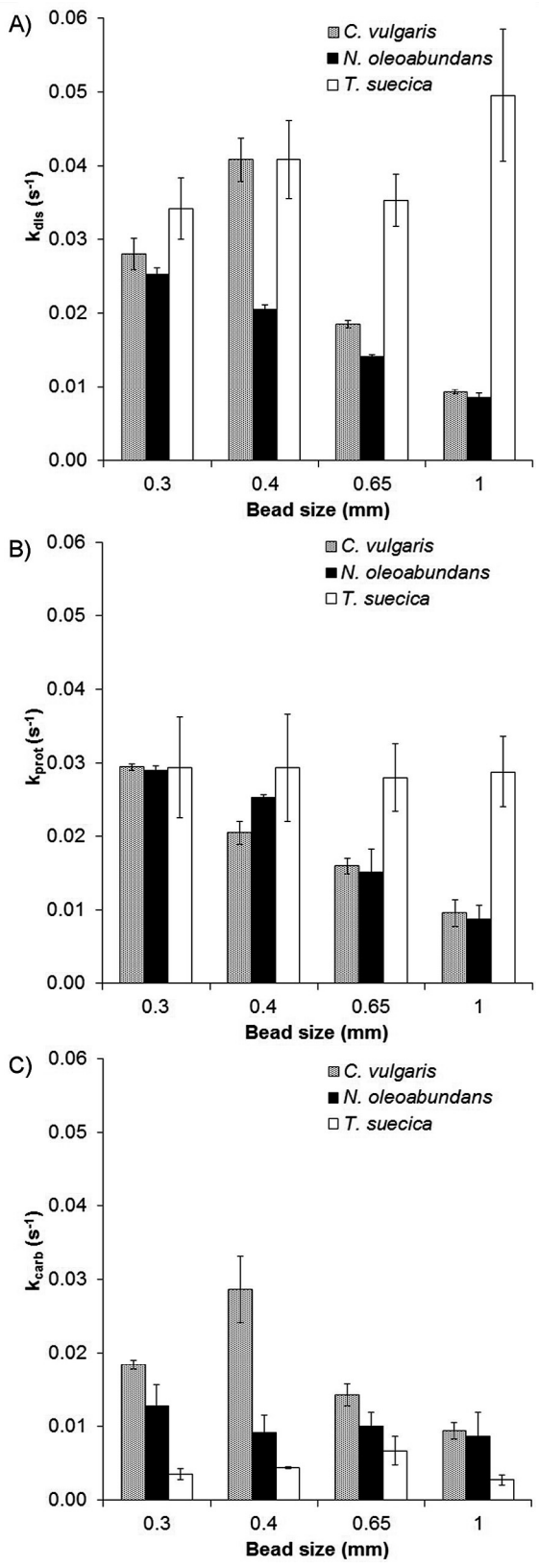

Fig. 2. Kinetic constants for disintegration k_{dis} (A), protein (B) and carbohydrate (C) release as a function of the bead size (mm) for *C. vulgaris*, *N. oleoabundans* and *T. suecica*.

to the bead size. The similar trends and magnitudes of k_{dis} and k_{prot} for all strains suggest that most of the proteins that were measured in the soluble phase are released to the bulk directly upon cell bursting. Differences in k_{dis} and k_{prot} are probably due to diffusion limiting transport. The absolute carbohydrate release rate was lower for *T. suecica* compared to *C. vulgaris* and *N. oleoabundans*. From the literature it is known that *T. suecica* can accumulate significant amounts of carbohydrates in the form of starch granules (Kermanshahi-pour et al., 2014), which are hardly soluble. For *T. suecica* the measured starch-carbohydrate ratio was always between 0.5 and 0.9, while for *C. vulgaris* and *N. oleoabundans* it was below 0.3 and 0.1, respectively.

Montalescot et al. (2015) observed no difference in the kinetic constant for bead diameters of 0.325 and 0.625 mm for the disintegration of the microalgae *N. oculata* (algae diameter 3 μm). Their reported value (k_{dis} of ~0.006 s^{-1}), however, is on average a factor 5–6 lower than the k_{dis} values obtained in the current study for similar bead sizes (0.3–0.65 mm).

3.2. Protein and carbohydrate yield

Different algae batches were used per bead size, and the composition (total protein, total carbohydrate and starch on biomass DW) of each batch was measured to calculate the product yield using Eq. (9); an overview is shown in Table 1.

According to Postma et al. (2015), 2.5–8 times more energy is required for continuing the bead milling process beyond 85–90% protein release in order to reach the maximum release. Therefore the yields in Fig. 3 are presented at 87.5% of the maximal release, which corresponds to 3τ (i.e., characteristic time of the protein/-carbohydrate release kinetic). τ can be described as:

$$\tau = k_i^{-1} \cdot \ln(2) \tag{11}$$

Considering the difference in protein and carbohydrate release kinetics, it is important to note that the time at which 87.5% release of each component is achieved is different for each species and bead size. For *C. vulgaris*, the highest water soluble protein yield (Fig. 3A) of 36.3% was obtained using 0.4 mm beads. For both *T. suecica* and *N. oleoabundans*, no significant differences ($p > 0.05$) between the protein yields were found at different bead sizes. The protein yields obtained for *C. vulgaris* using the 1 mm beads were similar to the yields found in previous work (Postma et al., 2015) under the same operating conditions.

Schwenzfeier et al. (2011) found a water-soluble protein yield of 21% using *Tetraselmis* sp., which is similar to the average yields found for *T. suecica* in this work. For *N. oleoabundans* under nitrogen replete cultivation conditions, up to 35% of water-soluble protein was released after bead milling (Günerken et al., 2016). In addition, 't Lam et al. (2016) found protein yields up to 50% after bead milling of *N. oleoabundans*. These studies, however, aimed at completed disintegration rather than optimizing energy consumption.

On average, a carbohydrate yield (Fig. 3B) of 62.7 ± 4.5% and 46.6 ± 17.2% was observed for *C. vulgaris* and *T. suecica*, respectively, independent of the bead size (based on Tukey's test). For *N. oleoabundans*, the carbohydrate yield improved ($p < 0.05$) from 22.4% to 40.3% from 1 mm to 0.3 mm, respectively. However, a clear trend could not be observed with decreasing bead sizes (Fig. 3B). Large variations in the carbohydrate yields were observed for *T. suecica*, which might be explained by natural variation or stress factors that altered the biomass composition. Analysis of the total starch content (Table 1) on biomass DW revealed that *T. suecica* contained considerably more starch with the same fluctuation as the yield, compared to *C. vulgaris* and *N. oleoabundans*. As was observed in the previous Section 3.1, the carbohydrate release kinetics behaved independent of the bead size and were not influenced by the biomass composition.

Table 1
Overview of biomass composition of *T. suecica*, *C. vulgaris* and *N. oleoabundans* for each bead milling experiment.

Experimental conditions		Biomass composition		
Algae	d_b (mm)	Protein $\%_{DW}$ ± SD	Carbohydrate $\%_{DW}$ ± SD	Starch $\%_{DW}$ ± SD
T. suecica	0.3	43.3 ± 2.7	21.2 ± 2.1	18.7 ± 0.1
	0.4	29.0 ± 0.0	33.7 ± 2.3	28.1 ± 0.9
	0.65	36.9 ± 0.3	16.0 ± 1.7	8.6 ± 0.1
	1	40.7 ± 3.5	23.6 ± 2.2	12.4 ± 0.2
C. vulgaris	0.3	53.1 ± 1.7	17.9 ± 0.6	4.6 ± 0.0
	0.4	57.0 ± 1.4	14.0 ± 0.7	2.8 ± 0.3
	0.65	53.4 ± 1.1	15.7 ± 0.3	5.3 ± 0.4
	1	51.6 ± 3.2	15.7 ± 0.4	3.4 ± 0.4
N. oleoabundans	0.3	47.3 ± 5.8	11.5 ± 2.1	1.3 ± 0.2
	0.4	50.8 ± 6.3	12.2 ± 1.3	1.0 ± 0.0
	0.65	51.2 ± 1.9	17.1 ± 2.5	1.5 ± 0.2
	1	55.6 ± 0.6	11.4 ± 1.7	0.9 ± 0.1

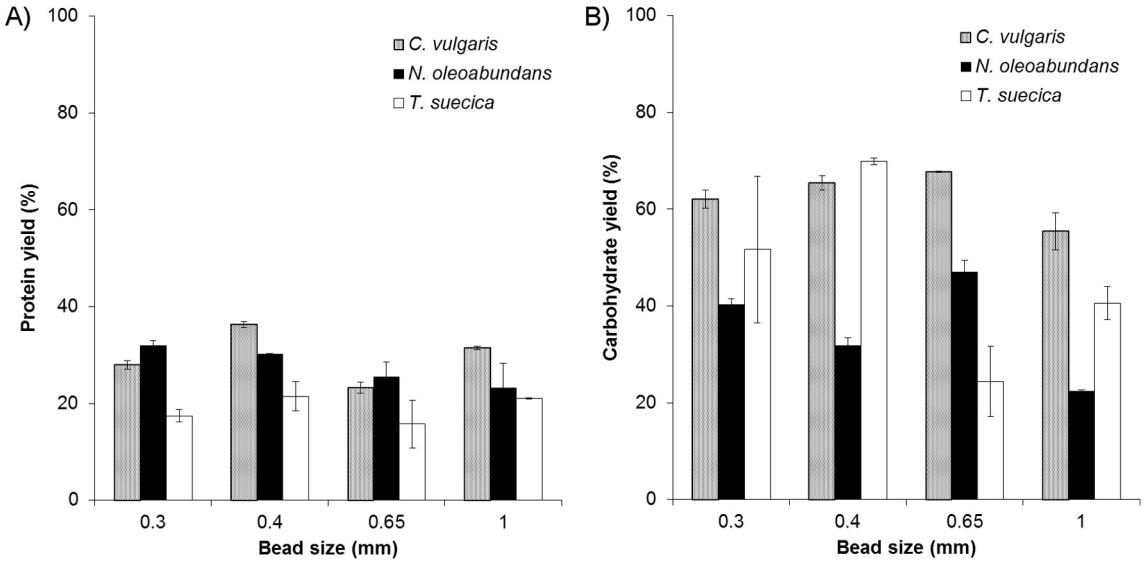

Fig. 3. Protein (A) and carbohydrate (B) yield as function of the bead size (mm). The shown protein and carbohydrate yield correspond to 87.5% of the maximal release (i.e. 3τ).

3.3. Disintegration mechanism

The disintegration of microalgae cells and the breakage of organelles and internal structures to release water-soluble biomolecules are the result of the shear generated by collisions of beads in the mill chamber. Using Eq. (4), the *SI* was calculated to be $5.8 \cdot 10^{-6}$, $1.4 \cdot 10^{-5}$, $5.9 \cdot 10^{-5}$ and $2.2 \cdot 10^{-4}$ Nm per bead for 0.3, 0.4, 0.65 and 1 mm beads, respectively. Since the same agitator tip speed and volumetric bead filling was used for each bead size, the total kinetic energy for each bead size should be equal, under the assumption that all beads acquire the agitator's tip speed. This explains the statistically similar rates observed for *T. suecica*, but cannot clarify why higher kinetic constants were measured at lower bead sizes for *C. vulgaris* and *N. oleoabundans*.

In this study, the SN (Eqs. (1) and (2)), which quantifies the amount of stress events during bead milling, is a function solely of bead size. The corresponding SN for the case of disintegrations (Eq. (1)) for all strains is presented in Fig. 4A–C. For *C. vulgaris* and *N. oleoabundans*, the disintegration percentage can be described by a single curve, independent of the bead size. For a constant stress number (e.g., $1 \cdot 10^7$), an increase in the bead size (i.e., increase in stress intensity) caused a larger disintegration percentage. This confirms the apparent trend (i.e., increased rate with increased bead size) in the disintegration kinetics (Fig. 2A). Furthermore, it shows that *SI* was below SI_{opt} because under the investigated bead diameters, bead sizes below 1 mm only gave the same level of disintegration when the stress number was increased.

When plotting the disintegration percentage as a function of the measured specific energy consumption E_M (Fig. 4D–F), the data for *T. suecica* are described by a single curve. Regardless of the bead size, the same energy is used to reach equal levels of disintegration. This is explained by the fact the specific energy consumption is proportional to the product of *SI* and *SN* (Eq. (5)). For *C. vulgaris* and *N. oleoabundans*, on the contrary, in order to achieve similar disintegration percentages with different beads, a higher energy consumption is required; for both algae, the small range of beads (0.3–0.4 mm) leads to the lowest energy consumptions (i.e., optimal energy utilization was achieved). Fig. 4 supports the idea that the cellular structure of *N. oleoabundans* (i.e., cell wall/membrane) presents higher resistance to shear damage, followed by *C. vulgaris* and *T. suecica*. Furthermore, Günther et al. (2016) reported the bursting energy for *C. vulgaris* in the range of $6.88 \cdot 10^{-3}$–$2.52 \cdot 10^{-4}$ kWh kg_{DW}^{-1} dry biomass and attributed this variation to differences in cell turgor and cell elasticity. The corresponding disintegration energy for *T. suecica* was $1.87 \cdot 10^{-4}$ kWh kg_{DW}^{-1} (one order of magnitude smaller) as estimated by Lee et al. (2013).

Scanning electron microscopy (SEM) micrographs of *C. vulgaris* were made prior to bead milling and after 50% and 87.5% disintegration using both 1 mm and 0.3 mm beads (Supplementary material Fig. A.1). Before disintegration, the cells have uniform spherical

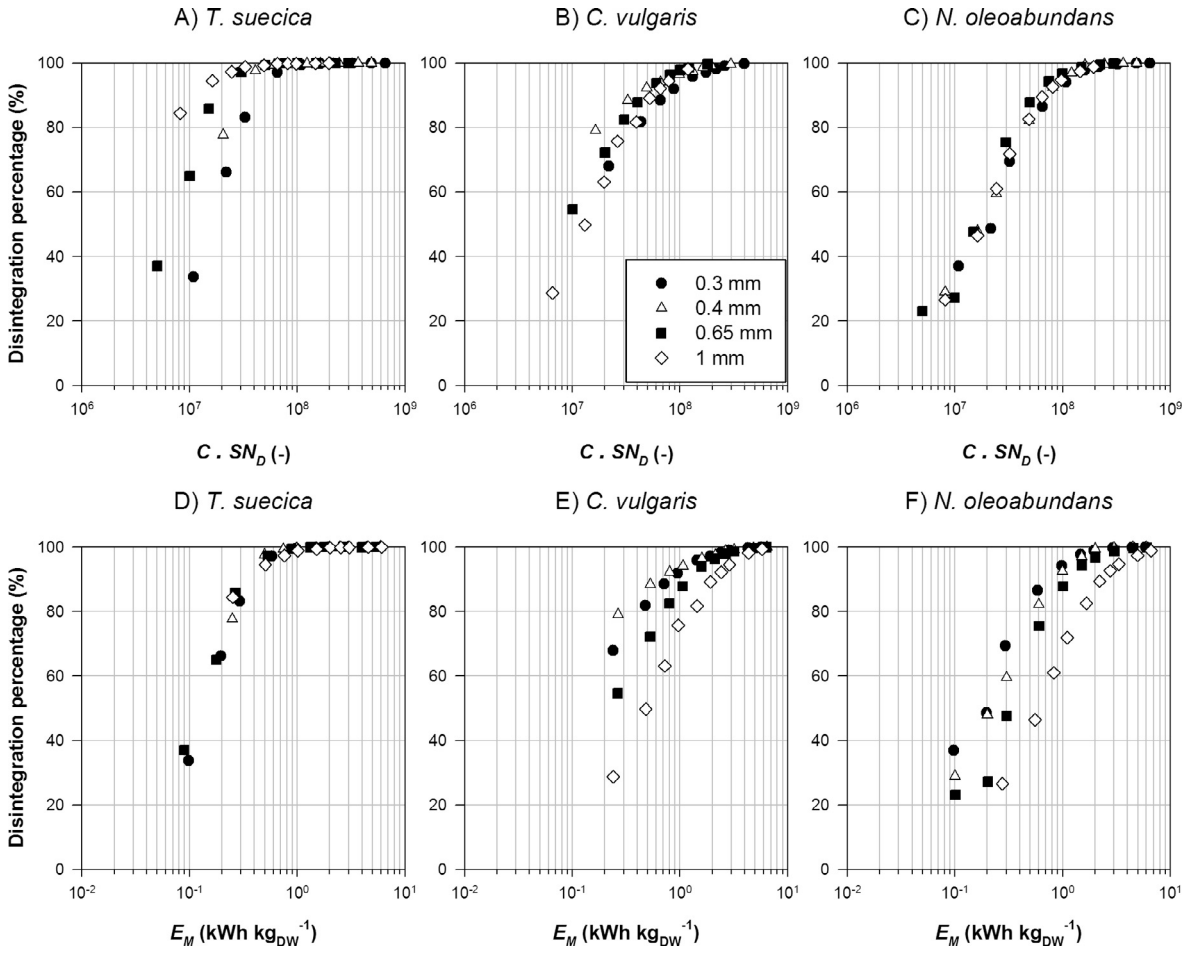

Fig. 4. Semi-log plot of disintegration percentage (%) as a function of stress number $C{\cdot}SN_D$ (–) for *T. suecica* (A), *C. vulgaris* (B) and *N. oleoabundans* (C). Semi-log plot of disintegration percentage as a function of the specific energy consumption E_M (kWh kg_{DW}^{-1}) for *T. suecica* (D), *C. vulgaris* (E) and *N. oleoabundans* (F).

shape, but appeared to be cracked upon bead impact after which the cell content was released, leaving an empty cell wall envelope. During disintegration, no visual differences could be observed in the breakage mechanism between bead sizes at the same disintegration rate of 87.5%.

For the release of proteins, a similar behavior was obtained with respect to the disintegration when plotting the fraction of release (normalized with respect to $Y_{Prot,\max}$ of individual experiment) versus the *SN* or E_M (Supplementary material Fig. A.2). This suggests that most of the soluble proteins are present in the cytoplasm or inside weak organelles. Upon disintegration, all proteins quickly migrate to the bulk medium. Conceptually, the process of protein release is similar to disintegration.

On the other hand, the release of carbohydrates revealed a different tendency (Supplementary material Fig. A.3). For all three algae species, the release of carbohydrates was found to depend on both *SN* and *SI* when plotting the release fraction versus $C{\cdot}SN_G$ (Supplementary material Fig. A.3A–C). Furthermore, it was observed that the release of carbohydrates can be described using the specific energy consumption at a first glance by a single curve (Supplementary material Fig. A.3D–F). Similar behavior was also observed for weak/medium-hard crystalline materials like limestone (Kwade and Schwedes, 2002), from which we hypothesize that carbohydrates from the cell wall and starch granules behave like crystalline material. During the course of the disintegration process the cell wall debris and starch granules are stressed multiple times, breaking off polymers, oligomers and monomers, thereby solubilizing simple sugars.

3.4. Specific energy consumption

The specific energy consumption for the release of 87.5% (3τ) of the maximal protein release ($E_{M,3\tau}$) for the benchmark set with *C. vulgaris* was 1.71 kWh kg_{DW}^{-1} (Postma et al., 2015). This was confirmed in the current work for *C. vulgaris* and *N. oleoabundans* (which behave similarly) with a specific energy consumption of 1.42 kWh kg_{DW}^{-1} and 1.78 kWh kg_{DW}^{-1}, respectively. An overview of τ and $E_{M,3\tau}$ is given in Table 2, in which it can be observed that *T. suecica* can give the same protein release regardless of the bead size using the same specific energy consumption on average 0.47 kWh kg_{DW}^{-1} ($p = 0.65$). In this regard, Lee et al. (2013) measured that the minimum specific energy $E_{M,min}$ required to break up one kg *T. suecica* is $1.87 \cdot 10^{-4}$ kWh kg_{DW}^{-1}, and compared it with an energy efficient disruption process (hydrodynamic cavitation) with an E_M of 9.2 kWh kg_{DW}^{-1} for a 1% w/w yeast suspension. In contrast, our findings (E_M: 0.47 kWh kg_{DW}^{-1}) show a twentyfold improvement of E_M compared to that process. Nonetheless, it is clear that mechanical disintegration methods are highly energy inefficient since a large fraction of the total energy is used to displace beads and fluid and another fraction is lost due to mechanical dissipation. According to Eq. (5), the specific energy consumption of the system is proportional to the *SI* and *SN*. The theoretical specific energy input of the beads $\tilde{E}_{M,3\tau}$ at 87.5% release of the protein content was calculated for each experiment. The ratio of $\tilde{E}_{M,3\tau}/E_{M,3\tau}$ gives an indication of how much energy was utilized to give the beads momentum and which part of the energy was dissipated. For 0.3, 0.4, 0.65 and 1 mm beads (for all algae), this ratio was below 1%,

Table 2
Overview of characteristic process time τ, specific energy consumption $E_{M,3\tau}$, protein concentration C_{Prot}, carbohydrate concentration C_{Carb} and selectivity S at 87.5% protein release.

Experimental conditions		Energy consumption		Product release		
Algae	d_b (mm)	$\tau \pm$ SD (s)	$E_{M,3\tau} \pm$ SD (kWh kg_{DW}^{-1})	$C_{Prot} \pm$ SD (g L^{-1})	$C_{Carb} \pm$ SD (g L^{-1})	S (C_{Prot}/C_{Carb})
T. suecica	0.3	24.3 ± 5.7	0.47 ± 0.11	6.7 ± 0.5	2.4 ± 0.7	2.8 ± 0.4
	0.4	24.4 ± 6.1	0.48 ± 0.12	5.7 ± 0.8	6.7 ± 1.5	0.9 ± 0.8
	0.65	25.1 ± 4.1	0.45 ± 0.07	5.3 ± 1.7	1.5 ± 0.3	3.4 ± 0.8
	1	24.4 ± 4.1	0.49 ± 0.06	7.7 ± 0.0	1.8 ± 0.0	4.4 ± 0.0
C. vulgaris	0.3	23.6 ± 0.3	0.45 ± 0.01	13.3 ± 0.4	8.3 ± 0.1	1.6 ± 0.2
	0.4	34.0 ± 2.6	0.72 ± 0.05	19.3 ± 0.3	9.2 ± 0.1	2.1 ± 0.2
	0.65	43.5 ± 2.9	0.92 ± 0.06	11.0 ± 0.6	9.1 ± 0.1	1.2 ± 0.3
	1	73.7 ± 13.7	1.42 ± 0.26	14.7 ± 0.2	7.8 ± 0.7	1.9 ± 0.4
N. oleoabundans	0.3	23.9 ± 0.5	0.47 ± 0.01	13.5 ± 0.5	2.8 ± 0.3	4.8 ± 0.3
	0.4	27.4 ± 0.4	0.55 ± 0.01	13.8 ± 0.0	2.1 ± 0.2	6.7 ± 0.1
	0.65	46.7 ± 9.4	0.94 ± 0.19	11.9 ± 1.4	6.3 ± 0.4	1.9 ± 0.7
	1	80.8 ± 17.3	1.78 ± 0.38	11.3 ± 2.5	2.2 ± 0.4	5.2 ± 1.3

2%, 5% and 11%, respectively, showing that the total required bead energy decreases with bead size. This might be caused by the increased probability of impact at lower bead sizes due to a high *SN* (i.e., more beads colliding in the mill) while maintaining an *SI* above SI_{opt}. Moreover, this shows that running a bead milling process close to SI_{opt} provides extra potential energy savings.

Fig. 4E, F shows that the energy utilization of the bead mill can be improved when smaller beads are applied during bead milling for *C. vulgaris* and *N. oleoabundans*. Decreasing the bead size from 1 to 0.3 mm can improve the energy utilization by a factor 3.3 and 3.9 ($p < 0.05$) for *C. vulgaris* and *N. oleoabundans*, respectively (Table 2). The lowest specific energy input found in this study was 0.45 kWh kg_{DW}^{-1} for *C. vulgaris* using a bead diameter of 0.3 mm resulting in a Y_{Prot} of 28% and a Y_{Carb} of 52%. Doucha and Lívanský (2008) reported energy consumptions between 2.8 and 10.0 kWh kg_{DW}^{-1} at 77.7% or 90.6% disintegration of *Chlorella* sp., though no product release was reported. Furthermore, $>55 \cdot 10^3$ - kWh kg_{DW}^{-1} was required for 90% disintegration of *N. oculata* by Montalescot et al. (2015). Safi et al. (2014) reported a Y_{prot} 49.6% for an E_M of 7.5 kWh kg_{DW}^{-1} for *C. vulgaris* using high pressure homogenization. In addition, Postma et al. (2016) reported an E_M of only 0.55 kWh kg_{DW}^{-1} for disintegration of *C. vulgaris* using pulsed electric field, though Y_p was below 5%.

With respect to the estimated energy content of a microalgae being 6.82 kWh kg_{DW}^{-1}, and the assumption that no more than 10% of the energy content of the algae should be used for extraction/-disintegration (National Algal Biofuels Technology Roadmap target, (U.S. DOE, 2010)), the total energy for extraction should not exceed 0.682 kWh kg_{DW}^{-1} (Coons et al., 2014). The $E_{M,3\tau}$ values presented in this work show that the specific energy consumption for bead milling can drop below this target, especially with the smaller 0.3 mm beads. To our knowledge, this is the first study to present such figures using fresh biomass.

As described above, it is known that mechanical disintegration techniques are energy inefficient processes in which a large part of the energy is not utilized for the effective breakage of cells. In a first assumption, the total energy is used to move parts (agitator), to displace beads and fluid, and dissipated into heat, which needs to be removed from the system by means of cooling. For the energy-efficient hydrodynamic cavitation process proposed by Lee et al. (2013), this means that only 0.002% of the required energy is utilized. Therefore, almost all energy needs to be removed as heat and thereby inevitably doubles the effective utilized energy. This would be true for all processes in which only an algae suspension is "moved" (e.g., high pressure homogenization, hydrodynamic cavitation, and ultrasound). However, in a bead milling process, not only is an algae suspension moved, but also the beads require energy to be displaced. The actual energy required for cooling of an algae suspension was also measured for *T. suecica*, using 0.4 mm beads and the conditions described in Section 2.2. During the course of one experiment (1 h) a ΔT of 18.2 °C was measured, which in terms of power, only corresponds to 4.2% of the E_M. Although the energy needed to cool down the engine is not yet included, it is evident that the cooling requirements could be ignored by running the bead milling shorter times (i.e., at 3τ) and by considering that after bead milling for 3τ (5 min) the suspension has heated up from 21.6 °C up to 24.3 °C, at which mild processing is still assured.

3.5. Selective protein release

An overview of the protein and carbohydrate concentration at 3τ protein release in the water-soluble phase is given in Table 2. *C. vulgaris* gives on average the highest absolute protein and carbohydrate concentration in the supernatant. High product concentrations are desirable if further fraction/purification is required, which reduces the amount of water that needs to be removed. Table 2 also provides an overview of the selectivity S (i.e., concentration ratio of released protein and released carbohydrate). In general, the process is selective towards proteins, in particular, at early stages of disruption ($S > 1$ for all times). The protein selectivity was highest for *N. oleoabundans*, followed by *T. suecica* and *C. vulgaris*. S can be regarded as a quality parameter for the bead milling process, i.e., a higher selectivity for the desired product makes further processing easier (e.g., less impurities). Therefore, S could be used to tune the desired properties of the end product. Schwenzfeier et al. (2011) found that "algae juice" (i.e., supernatant after bead milling), "crude protein isolate" and "purified protein isolate" from *Tetraselmis* sp. have good solubility at pH values (5.5–6.5), a range where seed protein isolates show low solubility. These extracts exhibit a selectivity factor of around 2. In addition, it was shown that the carbohydrate fraction contributes considerably to the high emulsion and foam stability over a large pH range (Schwenzfeier et al., 2014). This suggests that the protein-carbohydrate concentrates found in the current work might possess similar functionality.

The proteins released by bead milling were analyzed by means of Native PAGE to provide insight about the size of the released proteins and whether they were negatively affected (i.e., degradation or aggregation) (Fig. 5A–C). Overall, it can be observed that the microalgal proteins have a large size distribution. To investigate the hypothesis that smaller beads are favorable over larger beads to specifically release products from intracellular organelles, Rubisco (Ribulose-1,5-biphosphate carboxylase oxygenase) was chosen as a biomarker. Moreover, it is mainly located in an intracellular organelle called the pyrenoid (Meyer et al., 2012), which

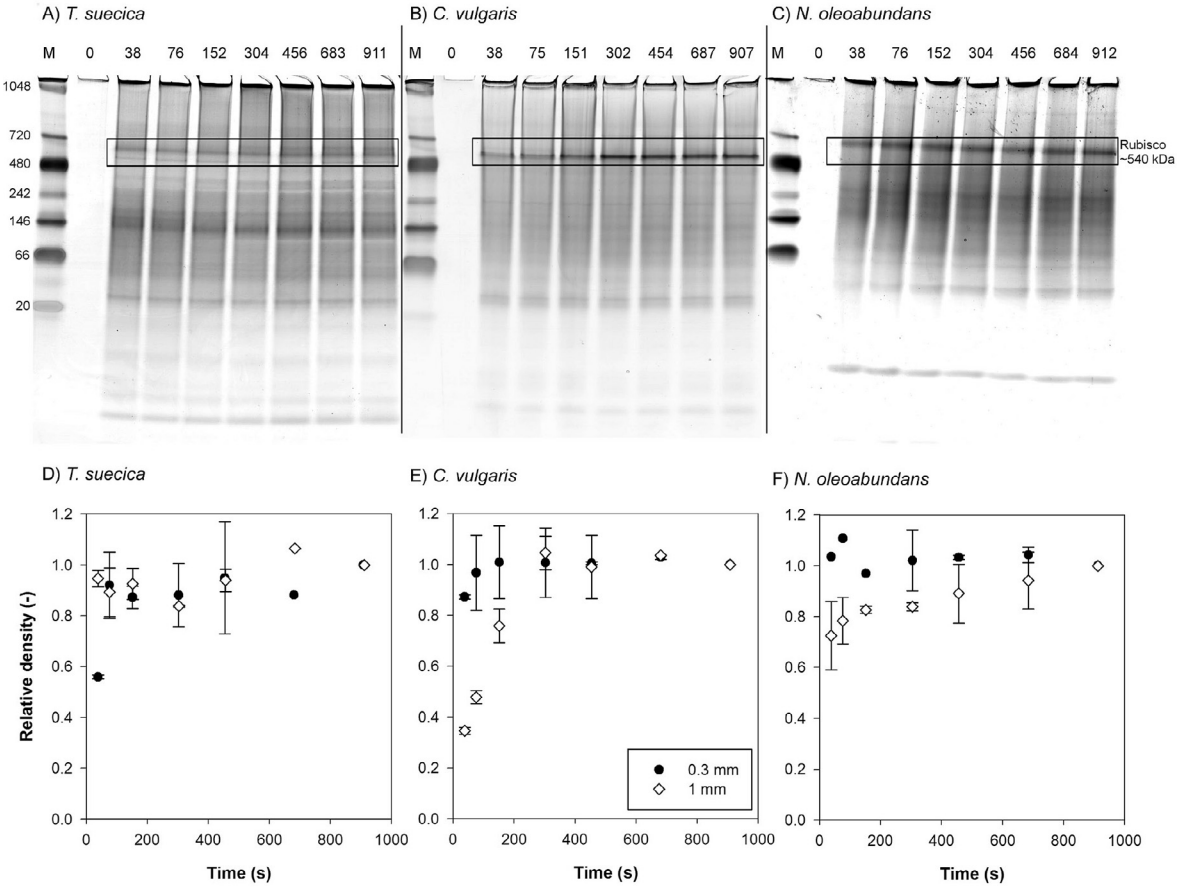

Fig. 5. Native PAGE gel after bead milling using 1 mm beads for *T. suecica* (A), *C. vulgaris* (B) and *N. oleoabundans* (C). Values on left in kDa, M: marker. Lanes are indicated by the time in s after start of bead milling. The black box marks the Rubisco band (~540 kDa). Relative density (–) versus time of bead milling (s) for *T. suecica* (D), *C. vulgaris* (E) and *N. oleoabundans* (F).

is present in the investigated strains. Rubisco consists of 8 large subunits (~56 kDa) and 8 small subunits (~14 kDa) making a native size of ~540 kDa. As can be observed from Fig. 5A–C, Rubisco is released over time during the bead milling process. The release of native and active Rubisco was also observed in a previous study (Postma et al., 2016).

The band intensities of Rubisco were graphically processed to a density chromatogram allowing peak identification and integration. With respect to the maximal amount of Rubisco obtained, a relative density plot was created (Fig. 5D–F). The most distinct difference was observed between the 1 mm and the 0.3 mm beads. With respect to the different microalgae used in this study, *T. suecica* (Fig. 5D) did not reveal any difference in the specific release of Rubisco. This could be due to the starch sheaths which *T. suecica* synthesizes around the pyrenoid structure, which make the pyrenoid not easily accessible (van den Hoek et al., 1995). Both *C. vulgaris* (Fig. 5E) and *N. oleoabundans* (Fig. 5F) showed that with a smaller bead size of 0.3 mm the release of Rubisco can be enhanced which further supports our hypothesis.

4. Conclusions

The kinetics of disintegration and component release was improved for *C. vulgaris* and *N. oleoabundans* at lower bead sizes, but remained unaffected for *T. suecica*, which appeared to be significantly weaker. For all strains, energy consumption was reduced to $\leqslant$0.47 kWh kg_{DW}^{-1} and the native structure of the released proteins was retained. Analysis of the stress parameters revealed that the bead mill was operated close to an optimum for *C. vulgaris* and *N. oleoabundans* at 0.3–0.4 mm beads. Finally, selective protein release was achieved in early stages of disintegration, for *C. vulgaris* and *N. oleoabundans*, using smaller beads.

Acknowledgements

We would like to thank Tiny Franssen-Verheijen of Wageningen University Electron Microscopy Centre for her help with the SEM, and Prof. Dr. Shirley Pomponi for proofreading of this manuscript. This project is conducted under the framework and financed by the IPOP Biorefinery from Wageningen University and Research Centre (The Netherlands) and the STW AlgaePro4U (nr. 12635). Part of this work was in cooperation with TKI AlgaePARC Biorefinery (nr. TKIBE01009).

Appendix A. Supplementary data

Supplementary data associated with this article can be found, in the online version, at http://dx.doi.org/10.1016/j.biortech.2016.11.071.

References

Balasundaram, B., Skill, S.C., Llewellyn, C.A., 2012. A low energy process for the recovery of bioproducts from cyanobacteria using a ball mill. Biochem. Eng. J. 69, 48–56.

Bunge, F., Pietzsch, M., Müller, R., Syldatk, C., 1992. Mechanical disruption of Arthrobacter sp. DSM 3747 in stirred ball mills for the release of hydantoin-cleaving enzymes. Chem. Eng. Sci. 47, 225–232.
CCAP, (Culture Collection of Algae and Protozoa), 2015. Bold's Basal Medium (BB).
Coons, J.E., Kalb, D.M., Dale, T., Marrone, B.L., 2014. Getting to low-cost algal biofuels: a monograph on conventional and cutting-edge harvesting and extraction technologies. In: Algal Res. 6 (Part B), 250–270.
Doucha, J., Lívanský, K., 2008. Influence of processing parameters on disintegration of Chlorella cells in various types of homogenizers. Appl. Microbiol. Biotechnol. 81, 431–440.
DuBois, M., Gilles, K.A., Hamilton, J.K., Rebers, P.A., Smith, F., 1956. Colorimetric method for determination of sugars and related substances. Anal. Chem. 28, 350–356.
Goettel, M., Eing, C., Gusbeth, C., Straessner, R., Frey, W., 2013. Pulsed electric field assisted extraction of intracellular valuables from microalgae. Algal Res. 2, 401–408.
Grimi, N., Dubois, A., Marchal, L., Jubeau, S., Lebovka, N.I., Vorobiev, E., 2014. Selective extraction from microalgae Nannochloropsis sp. using different methods of cell disruption. Bioresour. Technol. 153, 254–259.
Günerken, E., D'Hondt, E., Eppink, M.H.M., Garcia-Gonzalez, L., Elst, K., Wijffels, R.H., 2015. Cell disruption for microalgae biorefineries. Biotechnol. Adv. 33, 243–260.
Günerken, E., D'Hondt, E., Eppink, M., Elst, K., Wijffels, R., 2016. Influence of nitrogen depletion in the growth of N. oleoabundans on the release of cellular components after beadmilling. Bioresour. Technol. 214, 89–95.
Günther, S., Gernat, D., Overbeck, A., Kampen, I., Kwade, A., 2016. Micromechanical properties and energy requirements of the microalgae Chlorella vulgaris for cell disruption. Chem. Eng. Technol. n/a–n/a.
Halim, R., Rupasinghe, T.W.T., Tull, D.L., Webley, P.A., 2013. Mechanical cell disruption for lipid extraction from microalgal biomass. Bioresour. Technol. 140, 53–63.
Hedenskog, G., Enebo, L., Vendlová, J., Prokeš, B., 1969. Investigation of some methods for increasing the digestibility in vitro of microalgae. Biotechnol. Bioeng. 11, 37–51.
Kapaun, E., Reisser, W., 1995. A chitin-like glycan in the cell wall of a Chlorella sp. (Chlorococcales, Chlorophyceae). Planta 197, 577–582.
Kermanshahi-pour, A., Sommer, T.J., Anastas, P.T., Zimmerman, J.B., 2014. Enzymatic and acid hydrolysis of Tetraselmis suecica for polysaccharide characterization. Bioresour. Technol. 173, 415–421.
Kula, M.-R., Schütte, H., 1987. Purification of proteins and the disruption of microbial cells. Biotechnol. Prog. 3, 31–42.
Kwade, A., Schwedes, J., 2002. Breaking characteristics of different materials and their effect on stress intensity and stress number in stirred media mills. Powder Technol. 122, 109–121. Special issue i in Honour of Prof Jimbo.
Lamers, P.P., van de Laak, C.C.W., Kaasenbrood, P.S., Lorier, J., Janssen, M., De Vos, R. C.H., Bino, R.J., Wijffels, R.H., 2010. Carotenoid and fatty acid metabolism in light-stressed Dunaliella salina. Biotechnol. Bioeng. 106, 638–648.
Lee, A.K., Lewis, D.M., Ashman, P.J., 2013. Force and energy requirement for microalgal cell disruption: an atomic force microscope evaluation. Bioresour. Technol. 128, 199–206.
Lowry, O.H., Rosebrough, N.J., Farr, A.L., Randall, R.J., 1951. Protein measurement with the folin phenol reagent. J. Biol. Chem. 193, 265–275.
Meyer, M.T., Genkov, T., Skepper, J.N., Jouhet, J., Mitchell, M.C., Spreitzer, R.J., Griffiths, H., 2012. Rubisco small-subunit-helices control pyrenoid formation in Chlamydomonas. Proc. Natl. Acad. Sci. U.S.A. 109, 19474–19479.
Michels, M.H.A., Slegers, P.M., Vermuë, M.H., Wijffels, R.H., 2014. Effect of biomass concentration on the productivity of Tetraselmis suecica in a pilot-scale tubular photobioreactor using natural sunlight. Algal Res. Progress Perspect. Microalgal Mass Cult. 4, 12–18.
Montalescot, V., Rinaldi, T., Touchard, R., Jubeau, S., Frappart, M., Jaouen, P., Bourseau, P., Marchal, L., 2015. Optimization of bead milling parameters for the cell disruption of microalgae: process modeling and application to Porphyridium cruentum and Nannochloropsis oculata. Bioresour. Technol. 196, 339–346.
Postma, P.R., Miron, T.L., Olivieri, G., Barbosa, M.J., Wijffels, R.H., Eppink, M.H.M., 2015. Mild disintegration of the green microalgae Chlorella vulgaris using bead milling. Bioresour. Technol. Adv. Biofuels Chem. Algae 184, 297–304.
Postma, P.R., Pataro, G., Capitoli, M., Barbosa, M.J., Wijffels, R.H., Eppink, M.H.M., Olivieri, G., Ferrari, G., 2016. Selective extraction of intracellular components from the microalga Chlorella vulgaris by combined pulsed electric field–temperature treatment. Bioresour. Technol. 203, 80–88.
Safi, C., Charton, M., Ursu, A.V., Laroche, C., Zebib, B., Pontalier, P.-Y., Vaca-Garcia, C., 2014. Release of hydro-soluble microalgal proteins using mechanical and chemical treatments. Algal Res. 3, 55–60.
Schütte, H., Kroner, K.H., Hustedt, H., Kula, M.-R., 1983. Experiences with a 20 litre industrial bead mill for the disruption of microorganisms. Enzyme Microb. Technol. 5, 143–148.
Schwenzfeier, A., Wierenga, P.A., Gruppen, H., 2011. Isolation and characterization of soluble protein from the green microalgae Tetraselmis sp. Bioresour. Technol. 102, 9121–9127.
Schwenzfeier, A., Wierenga, P.A., Eppink, M.H.M., Gruppen, H., 2014. Effect of charged polysaccharides on the techno-functional properties of fractions obtained from algae soluble protein isolate. Food Hydrocolloids 35, 9–18.
't Lam, G.P., Postma, P.R., Fernandes, D.A., Timmermans, R.A.H., Vermue, M.H., Barbosa, M.J., Eppink, M.H.M., Wijffels, R.H., Olivieri, G., 2016. Pulsed electric field for protein release of the microalgae Chlorella vulgaris and Neochloris oleoabundans (submitted for publication), submitted to Algal Research (ALGAL_2016_122).
U.S. DOE, 2010. National Algal Biofuels Technology Roadmap. U.S. Department of Energy, Office of Energy Efficiency and Renewable Energy, Biomass Program.
van den Hoek, C., Mann, D., Jahns, H.M., 1995. Algae: An Introduction to Phycology. Cambridge University Press.
Vanthoor-Koopmans, M., Wijffels, R.H., Barbosa, M.J., Eppink, M.H.M., 2013. Biorefinery of microalgae for food and fuel. Bioresour. Technol. 135, 142–149.